

LOSS OF ADHESION OF A LAYER BONDED TO AN ELASTIC HALF SPACE CAUSED BY A CONCENTRATED CONTACT

Sung-Ho Kim*, Leon Keer** and Herbert Cheng**

(Received March 24, 1989)

A model is constructed to analyze the effects of a concentrated contact on a layer that is perfectly bonded to an elastic half space, except for a debond region, which is analyzed as a frictional interfacial crack. The crack is assumed not to open and the growth is governed by a mode II stress intensity factor that is retarded by interfacial friction. This model may be used to study the fracture of hard coatings at the asperity scale where the failure is caused by loss of adhesion at the interface.

Key Words : Contact, Interfacial Crack, Mode II Stress Intensity Factor, Coating

NOMENCLATURE

a	: Half of contact length
$b(x)$: Tangential dislocation density
d	: Half of crack length
f_1	: Frictional coefficient of the indenter
f_2	: Frictional coefficient of the crack
H	: Thickness of the layer
H_0	: Layer thickness corresponding to H_0/a_0 of 0.53 (maximum interfacial shear stress occurs at $H_0/a_0 \approx 0.53$ for the case of tungsten coated to steel)
ν_j	: Poisson's ratio
χ_j	: Muskhelishvili constant
	$\left\{ \begin{array}{l} \chi_j = (3 - \nu_j) / (1 + \nu_j) \text{ for plane stress} \\ \chi_j = 3 - 4\nu_j \text{ for plane strain} \end{array} \right.$
L	: Crack length
μ_j	: Shear modulus
Γ	: Shear modulus ratio of the layer to the substrate (μ_1/μ_0)
λ	: Ratio of half length of crack to the layer thickness ($L/2H$)
$p(x)$: Surface pressure
t	: Distance from the center of the crack to the center of the loading
K_L, K_T	: Mode II stress intensity factors of the leading tip, trailing tip
$S(x), T(x)$: Normal and shear tractions
u_j, v_j	: Displacement components
$\sigma_{xy(j)}, \sigma_{yy(j)}, \sigma_{xx(j)}$: Stress components

Subscripts

$i=1$: Layer, $i=0$: Substrate

1. INTRODUCTION

Some of the more important reasons for using a hard coating are to obtain better wear resistance, physical prop-

erties (conductivity, reflectance, color, etc.), corrosion resistance and to improve the range of load tolerance. For example, ceramic coatings have been used extensively to increase the wear resistance in many tools and machine elements. At present, there is very little analytical guidance to direct the engineer towards choosing the optimum coating thickness for long fatigue life.

A hard coating may be a layer whose yield strength is much higher than the substrate. The deformation throughout the layer-substrate combination can be made elastic provided that the thickness of the layer is chosen sufficiently large that the peak Mises stresses occur there and decrease with depth to such magnitudes that substrate yielding will not occur. In the particular case for thick TiN layers ($H/a > 1$) deposited on titanium and steel, the Mises stresses normalized to the yield stress of the layer can be markedly reduced within the hard layer and thus, yielding in the layer-substrate combination can be prevented (Komvopoulos, 1987). Also, it was found from experiment that $0.8\mu\text{m}$ thickness of the TiN layers was sufficient to eliminate yielding at and below the layer-substrate interface (Komvopoulos, 1987). Although yielding may be prevented in the substrate by thick layers, delamination may occur if the critical interfacial shear strength is exceeded. For thin layers the peak stresses probably occur in the substrate and increasing the thickness could bring these damaging stresses to the interface.

The analysis of hard coatings therefore requires careful study of the adhesive properties that bind the coating to the substrate. Since a major effect of a concentrated contact will be to stress the interface between the coating and the substrate in shear, a first step is to study the effects of a debonding at the interface and its tendency to propagate. It is noted that if the extent of contact is of the same order as the thickness of the coating, then from size considerations the analysis will be appropriate for the asperities that comprise the concentrated contact when the coating is thin (less than $1\mu\text{m}$).

To analyze the effects of crack face friction on growth, McClintock (McClintock, 1977) introduced the concept of the net tip shear stress, which is the stress available to produce the stress intensity factors at the crack tips. He considered a

*Agency for Defense Development, Taejeon, 300-600 Korea.

**Department of Mechanical Engineering, Northwestern University, Evanston, Illinois, 60201, U.S.A.

short crack whose net tip shear stress was approximated as constant over the entire crack face. Hearle and Johnson (Hearle and Johnson, 1985) developed a Green's function model for relatively long subsurface cracks which have stick and slip regions in a single crack. They found that the range of mode II stress intensity factors experienced by the trailing tip of a subsurface crack is larger than that of the leading tip for relatively long cracks ($H/d < 1$). From that, they further observed the rolling direction as a possible mechanism in the propagation of rolling contact fatigue cracks.

As a preliminary study to the problem of a moving load, Chang et al. (Chang et al., 1984) considered the static problem of an elastic layer pressed onto an identical substrate. They included a uniform compressive surface load to prevent the possibility of developing subsurface tension, which causes the opening of the crack. Also, Sheppard et al. (Sheppard et al., 1985) studied a moving load for a half space.

This study extends their reasoning to the case of an interfacial crack between an elastic layer and dissimilar elastic half space, when the surface of the layer is subjected to a sliding point load and to a rigid indentation. The crack is assumed not to open and the growth is governed by a mode II stress intensity factor which is retarded by the presence of the interfacial crack face friction. This model may be used to study the fracture of hard coatings where the failure mechanism is loss of the interfacial adhesion. In this analysis several important parameters associated with possible layer debond have been studied such as crack face friction, crack length, the stiffness ratio of the layer and substrate, and size of contact relative to layer thickness. In the sequel the assumption is made that the debond length is sufficiently small that only one slip zone will occur.

2. BASIC EQUATIONS AND DERIVATIONS

An analytical model is derived for a concentrated line contact of an elastic layer which is perfectly bonded to a dissimilar half space except for a small region of debond, which is analyzed as an interfacial crack. In Fig. 1 and for the rest of this study subscripts 1 and 0 refer to the layer and the half space, respectively. To obtain the desired solution, a superposition of the two following solutions is utilized: (1) A concentrated contact of an elastic layer perfectly bonded to a half space (Fig. 2), (2) A gliding-type edge dislocation in the layer substrate interface (Fig. 3). The boundary conditions for the overall problem are the following:

Boundary Conditions

$$\sigma_{xy(1)} = -f_1 \sigma_{yy(1)} \quad y = -H \quad (1)$$

$$\sigma_{yy(1)} = -p(x) \quad y = -H \quad (2)$$

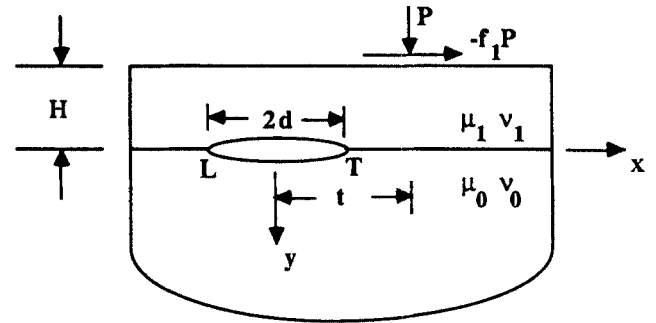
$$\sigma_{yy(1)} = \sigma_{yy(0)} \quad y = 0 \quad (3)$$

$$\sigma_{xy(1)} = \sigma_{xy(0)} \quad y = 0 \quad (4)$$

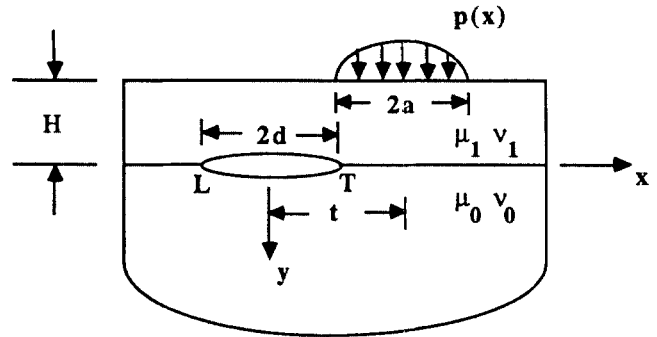
$$v_1 = v_0 \quad y = 0 \quad (5)$$

$$\frac{\partial}{\partial x}(u_1 - u_0) = \begin{cases} 0, & x < -d \text{ or } x > d \\ b(x), & -d < x < d \end{cases} \quad y = 0 \quad (6)$$

The concentrated contact problem of a layer with perfect bonding to a half space can be achieved by making $b(x) = 0$, whereas the problem of a gliding-type edge dislocation with free boundary in the layer can be achieved by making $p(x) = 0$. Hearle and Johnson (Hearle and Johnson, 1985) note that a point load (Fig. 1a) produced very close subsurface stress



(a) Concentrated contact with interfacial crack



(b) Hertzian contact with interfacial crack

Fig. 1

distributions to a Hertzian load (Fig. 1b) when the contact radius is relatively small ($2a/H < 1$). Suitable elasticity solutions for these two problems are as follows:

2.1 Hertzian Contact with Perfect Bonding

$$2\mu_j u_j = i \int_{-a}^a p(s) ds \int_{-\infty}^{\infty} \xi L_j(\xi, y) B_1(\xi) e^{-i\xi(x-s)} d\xi \quad (7)$$

$$2\mu_j v_j = \int_{-a}^a p(s) ds \int_{-\infty}^{\infty} \xi |M_j(\xi, y) B_1(\xi) e^{-i\xi(x-s)} d\xi \quad (8)$$

$$\sigma_{yy(j)} = \int_{-a}^a p(s) ds \int_{-\infty}^{\infty} \xi^2 N_j(\xi, y) B_1(\xi) e^{-i\xi(x-s)} d\xi \quad (9)$$

$$\sigma_{xy(j)} = i \int_{-a}^a p(s) ds \int_{-\infty}^{\infty} \xi |P_j(\xi, y) B_1(\xi) e^{-i\xi(x-s)} d\xi \quad (10)$$

$$\sigma_{xx(j)} = \int_{-a}^a p(s) ds \int_{-\infty}^{\infty} \xi^2 R_j(\xi, y) B_1(\xi) e^{-i\xi(x-s)} d\xi \quad (11)$$

$$\begin{cases} j=0 : \text{the half space} \\ j=1 : \text{the layer} \end{cases}$$

Here, μ_j is the shear modulus, $\alpha_j = 3 - 4\nu_j$ for plane strain and $\alpha_j = (3 - \nu_j)/(1 + \nu_j)$ for plane stress, ν_j being Poisson's ratio, and B_1 , L_j , M_j , N_j , P_j and R_j are defined in the Appendix.

2.2 Loading at Interfacial Crack

$$2\mu_j u_j = i \int_{-\infty}^{\infty} \xi D_j(\xi, y) B_0(\xi) e^{-i\xi x} d\xi \quad (12)$$

$$2\mu_j v_j = \int_{-\infty}^{\infty} \xi |E_j(\xi, y) B_0(\xi) e^{-i\xi x} d\xi \quad (13)$$

$$\sigma_{yy(j)} = \int_{-\infty}^{\infty} \xi^2 F_j(\xi, y) B_0(\xi) e^{-i\xi x} d\xi \quad (14)$$

$$\sigma_{xy(j)} = i \int_{-\infty}^{\infty} \xi |G_j(\xi, y) B_0(\xi) e^{-i\xi x} d\xi \quad (15)$$

$$\sigma_{xx(j)} = \int_{-\infty}^{\infty} \xi^2 H_j(\xi, y) B_0(\xi) e^{-i\xi x} d\xi \quad (16)$$

$$\begin{cases} j=0 : \text{the half space} \\ j=1 : \text{the layer} \end{cases}$$

Here, B_0 , D_j , E_j , F_j , G_j and H_j are defined in the Appendix.

2.3 Hertzian Contact with Interfacial Crack

Due to the compression produced by the asperity and global Hertzian contacts, the crack is assumed not to open; it will either stick or slip as the load moves along the positive x direction with the region of stick or slip depending mainly upon the crack face friction and the crack length. The normal $N(x)$ and shear $S(x)$ tractions on $y=0$ are

$$\begin{aligned} N(x) &= \frac{2\mu_0}{\pi(x_0+1)(1-\beta^2)} \{-\beta(1+\alpha)\pi b(x) \\ &\quad + \int_{-a}^a b(\xi) K_1^p(\xi, x) d\xi\} - \frac{1}{2\pi} \int_{-a}^a p(s) \\ &\quad K_1^f(s, x) ds \\ S(x) &= \frac{2\mu_0}{\pi(x_0+1)(1-\beta^2)} \{(1+\alpha) \int_{-a}^a \frac{b(\xi) d\xi}{\xi-x} \\ &\quad + \int_{-a}^a b(\xi) K_2^p(\xi, x) d\xi\} - \frac{1}{2\pi} \int_{-a}^a p(s) \\ &\quad K_2^f(s, x) ds \end{aligned} \quad (17-18)$$

where, α and β are Dundurs' constants (Dundurs, 1969; Dundurs, 1970) and $K_1^f(s, x)$, $K_2^f(s, x)$ are the stress kernels for undisturbed system, $K_1^p(\xi, x)$ and $K_2^p(\xi, x)$ are stress kernels for the dislocation system which are defined in the Appendix. The first terms in (17) and (18) are due to the gliding-type edge dislocation (corrective solution) and the remaining terms are due to the surface load (undisturbed solution). We assume Coulomb friction in the slip zones as

$$|S(x)| = f_2 \operatorname{sgn}(x) N(x) \quad \text{in } \Sigma \quad (19)$$

$$N(x) \leq 0 \quad \text{in } \Sigma \quad (20)$$

where, f_2 is the crack face friction and Σ is the slip zone. Accordingly, in the slip zones, we have following Cauchy integral equation of a second kind as

$$\begin{aligned} (1+\alpha) \int_{-a}^a \frac{b(\xi)}{\xi-x} d\xi - \beta(1+\alpha)\pi b(x) \\ + \int_{-a}^a b(\xi) [K_2^p(\xi, x) + f_2 \operatorname{sgn}(x) K_1^p(\xi, x)] d\xi \\ = -\frac{(x_0+1)(1-\beta^2)}{4\mu_0} \int_{-a}^a p(s) [K_2^f(s, x) \\ + f_2 \operatorname{sgn}(x) K_1^f(s, x)] ds \quad \text{in } \Sigma \end{aligned} \quad (21)$$

Additionally, since the crack is closed at the endpoints,

$$\int_{-a}^a b(\xi) d\xi = 0 \quad (22)$$

In the stick zone

$$|S(x)| < -f_2 N(x) \quad (23)$$

$$N(x) \leq 0 \quad (24)$$

The dislocation density remains fixed in the stick zone as the crack advances. To solve (21), after making the following nondimensional definitions

$$\begin{aligned} x/H = \lambda \bar{x}, \quad \xi/H = \lambda \bar{\xi}, \quad s/H = a/H \bar{s}, \quad t/H = a/H \bar{t}, \\ p(x) = \frac{4\mu_0}{(x_0+1)} \bar{p}(\bar{x}) \end{aligned} \quad (25)$$

a weight function method for solving the Cauchy-type singular integral equation of a first kind is used; when the loading

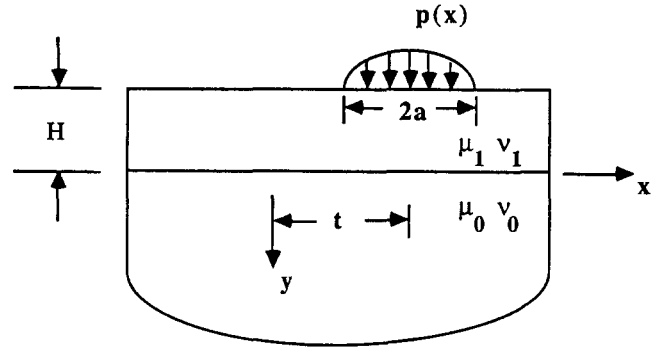


Fig. 2 Hertzian contact with perfect interfacial bonding

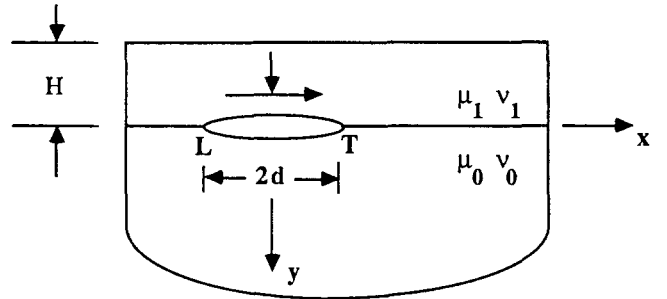


Fig. 3 Loading at interfacial crack

surface is frictionless, the solution is expressed as $b(x) = \phi(x)(1-x^2)^{-1/2}$ (Miller and Keer, 1985). Once the integral equation is solved, the crack tip stress intensity factors in the Fourier integral transform domain may be readily calculated as

$$(K_{II})_L = \frac{2(1+\alpha)\sqrt{\lambda}\mu_0\sqrt{d}}{(x_0+1)(1-\beta^2)} \phi(-1) \quad (26)$$

$$(K_{II})_T = -\frac{2(1+\alpha)\sqrt{\lambda}\mu_0\sqrt{d}}{(x_0+1)(1-\beta^2)} \phi(1) \quad (27)$$

Here, the subscripts L and T represent leading and trailing crack tips respectively as shown in Fig. 1 and Fig. 3. Also, $(K_{II})_L$ is the stress intensity factors of the leading tip where the region of slip and lock is assumed to be determined by the relative location of the leading crack tip to the surface load, and $(K_{II})_T$ is the stress intensity factors of the trailing tip to the surface load, and $(K_{II})_T$ is the stress intensity factors of the trailing tip where the region of slip and lock is assumed to be determined by the relative location of the trailing tip to the surface load. This assumption cannot account for the growing slip and stick zone, however when the crack is short relatively to the layer thickness the difference with derives from that is small enough to be neglected (Sheppard et al., 1985). Guided by a problem of a crack extending from $-\infty$ to $+\infty$ when the layer is pressed on a substrate (Comninou et al., 1980), the lock starts x^* as the load moves along the positive x direction where,

$$x^*/H = -\frac{1}{3} [(3+4f_2^2)^{1/2} + 2f_2] \quad (28)$$

It should be noted that the location of slip and lock boundary depends only upon the coefficient of the crack face friction not the magnitude of the concentrated load because of the absence of the uniform load. For example, slip occurs for

$x/H < -1$ and lock starts at $x/H = -1$ as the load moves when $f_1 = 0.5$. For a finite length crack similar behavior is expected. As long as the loading is applied to a final value without unloading before the first locking zone is reached during the passage of a load, the slip for the first stage is independent of loading sequence. In this analysis only short crack ($L/H = 0.25$) is considered so that the stress distribution on the crack face is assumed to be approximately as constant.

3. NUMERICAL RESULTS

The mode II stress intensity factor is calculated first when the layer is subjected to a moving point load. This calculation is appropriate for layers which are thick compared to the contact region or asperity dimension. The number of possible slip zones can be determined by the magnitude of the crack face friction and the crack length. Sheppard et al. (Sheppard et al., 1985) found that a crack whose length is shorter than the layer thickness has only one slip zone, while a crack whose length is longer than the layer thickness has two slip zones in a single crack when the crack face friction is assumed to be 0.5. The size and the location of the slip and stick regions and also the range of the stress intensity factors depend largely upon the crack face friction and the crack length. Fig. 4 shows that the maximum and minimum values of the stress intensity factors at crack tips L and T are almost identical when the crack length L/H is less than 0.25 (Sheppard et al., 1985). The validity of this assessment deteriorates somewhat when the crack friction is very small. Numerical results in this analysis match well with their

results when $L/H = 0.25$.

In this analysis, cracks whose lengths are short enough to produce only one slip zone are considered. The case for which numerical results will be given is that of a tungsten coating on a steel base which represents a hard coating whose shear modulus is twice stiffer than that of the substrate. Fig. 5 and 6 are the mode II stress intensity factors experienced by a passage of moving load. While the crack stays locked there is no change of displacements along the crack so that stress intensity factors at the tips remain constant. Therefore, the flat part of the line in the figures represents a locked region. The stress intensity factors are asymmetric with respect to t because of the history dependency of the problem. As the crack face friction increases from 0 to 0.7, the range of stress intensity factors decreases significantly as does the size of the slipped region. Generally, the friction coefficient depends upon the combinations of the materials and can be as high as 0.7 or 0.8 (Yoshimura, Rubin and Hahn, 1984) which causes a significant reduction of stress intensity factors. For very short cracks ($L/H = 0.25$) with crack face friction $f_2 = 0.5$, the stress intensity factors of the leading tip and trailing tip are almost identical during the entire passage of a load except near the region of the slip and stick boundaries.

Next, the case where the surface is loaded by a finite length contact at the asperity scale is studied. For many industrial applications a single asperity contact length may be approx-

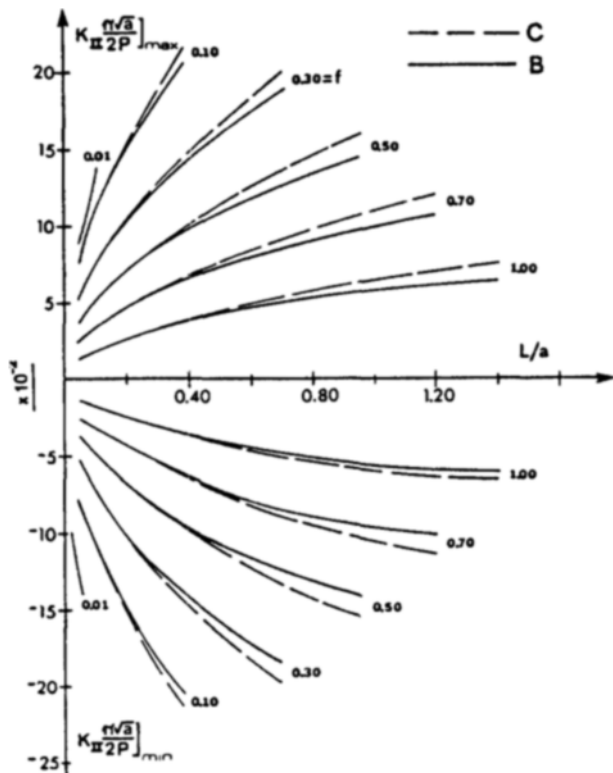


Fig. 4 Maximum and minimum values of stress intensity factors at B and C as functions of crack length L/a for various coefficient of friction (Sheppard et al., 1985)

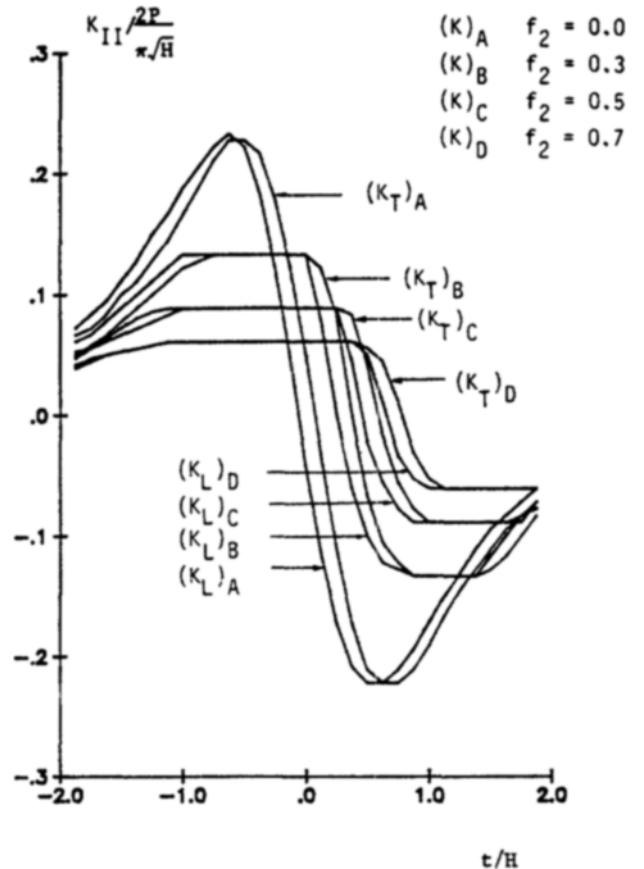


Fig. 5 K_{II} of the crack tips relative to the point of load application ($f_1 = 0.0, L/H = 0.25$)
Material 1: Steel
Material 0: Steel

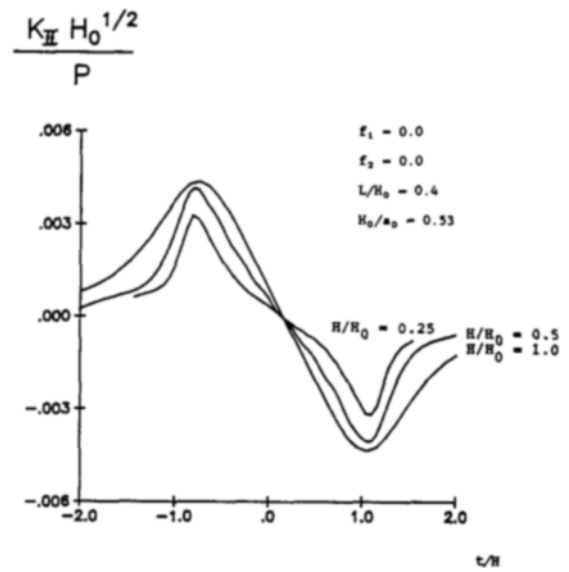
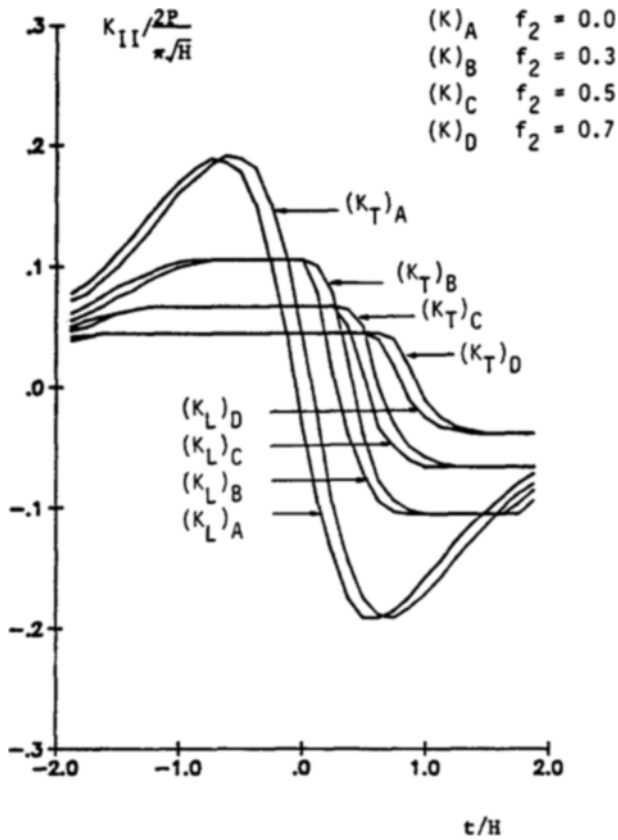


Fig. 8 Effect of coating thickness on the stress intensity factors ($\mu_1/\mu_0=2.0$)
Material 1: Tungsten
Material 0: Steel

thickness on the interfacial shear stress for a typical asperity contact of a contact length $2a$ and load P . Fig. 7 shows the influence of coating thickness on the non-dimensional interfacial shear stress, $\sigma_{xy}H_0/P$, where σ_{xy} is the interfacial shear stress, H_0 is the coating thickness corresponding to a coating thickness to contact length ratio H_0/a_0 of 0.53 when the layer is tungsten and the substrate is steel (The maximum interfacial stress will occur at $H_0/a_0 \approx 0.53$). Fig. 8 shows the effect of coating thickness on the stress intensity factors for a frictionless crack. Qualitatively similar behavior to the previous cases is expected for cracks with friction. Both the interfacial shear and stress intensity factors are seen to increase with the coating thickness for $H/H_0 < 1$, and decrease with the coating thickness for $H/H_0 > 1$. Therefore, it is concluded that the layer thickness should be designed to be sufficiently thin to minimize the interfacial shear stress and assure a good interfacial bond. However, when $H/H_0 < 1$ the maximum Mises stresses lie in the substrate thereby posing the possibility of yielding and crack initiation. It is up to the designer to decide which of these possibilities is critical for the component's use.

ACKNOWLEDGEMENT

The authors are grateful for the support of the Center for Engineering Tribology, at Northwestern University, funded by NSF under Grant No. ISI-8415521 and an industrial consortium including sixteen U.S. companies.

REFERENCES

Chang, F.K. et al., 1984, "The Subsurface Crack Under Conditions of Slip and Stick Caused by a Surface Normal Load", J. Appl. Mech., Vol. 51, pp. 311~316.
Comninou, M., Schmueser, D. and Dundurs, J., 1980, "Fric-

Fig. 6 K_{II} of the crack tips relative to the point of load application ($f_1=0.0, L/H=0.25$)
Material 1: Tungsten
Material 0: Steel

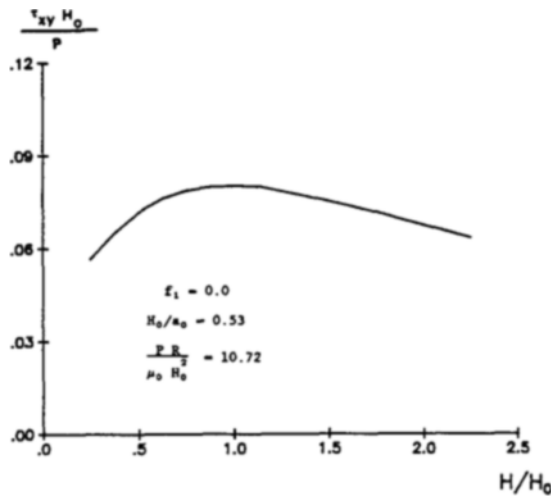


Fig. 7 Effect of coating thickness on the peak interfacial shear stress ($\mu_1/\mu_0=2.0$)
Material 1: Tungsten
Material 0: Steel

imated as 20~40 μ m while the coating thickness can range from 0.5 to 5 μ m. Therefore, ratios of layer thickness to the contact length (H/a) ranging from 0.125 to 1.25 are examined here. The most significant finding is the effect of coating

tional Slip Between a Layer and Substrate Caused by a Normal Load", Int. Journal of Engineering Science, Vol. 18, pp. 131~137.

Dundurs, J., 1969, "Discussion of a Paper by D.B. Bogy", Journal of Applied Mechanics, Vol. 36, pp. 650~652.

Dundurs, J., 1970, "Some Properties of Elastic Stresses in a Composite", Recent Advances in Engineering Science(ed. A. C. Eringen), Gordon & Breach, Vol. 5, pp. 203~216.

Hearle, A.D. and Johnson, K.L., 1985, "Mode II Stress Intensity Factors for a Crack Parallel to the Surface of an Elastic Half Space Subjected to a Moving Point Load", J. Mech. Phys. Solids, Vol. 33, pp. 61~68.

Komvopoulos, K., Saka, N. and Suh, N.P., 1987, "The Role of Hard Layers in Lubricated and Dry Sliding", Journal of Tribology, Vol. 109, pp. 223~231.

McClintock, F.A., 1977, "Plastic Flow Around a Crack under Friction and Combined Stress", Advances in Research on the Strength and Fracture of Materials, edited by D.M.R. Taplin, Pergamon, Vol. 4, pp. 23~28.

Miller, G. and Keer, L.M., 1985, "A Numerical Technique for the Solutions of Singular Integral Equations of the Second Kind", J. Appl. Math., Vol. 42, pp. 455~465.

Sheppard, S., Barber, J.R. and Comninou, M., 1985, "Short Subsurface Cracks under Conditions of Slip and Stick Caused by a Moving Compressive Load", J. Appl. Mech., Vol. 52, pp. 811~817.

Yoshimura, H., Rubin, C.A. and Hahn, G.T., 1984, "Crack Initiation and Cyclic Crack Growth in AISI 4140 Steel and 7075-T6 Aluminum Alloys under Repeated Rolling Contacts", Preliminary draft prepared for publication at a later date.

APPENDIX

$$\begin{aligned}
 B_1(\xi) &= \frac{(1-\beta)^2 e^{\xi H} - (\alpha-\beta)(1+\beta)(1-2\xi H) e^{-\xi H}}{\Delta} \\
 Q_1 &= \frac{(1+\beta)(\alpha-\beta)(1+2\xi H) e^{\xi H} - (\alpha^2-\beta^2) e^{-\xi H}}{(1-\beta^2) e^{\xi H} - (1-2\xi H)(1+\beta)(\alpha-\beta) e^{-\xi H}} \\
 L_1 &= \frac{1}{4\pi} \left[(2z-x_1) e^{-z} - \frac{\alpha+\beta}{1+\beta} e^z \right. \\
 &\quad \left. + Q_1 \left\{ \frac{1-\beta}{\alpha-\beta} e^{-z} + (2z+x_1) e^z \right\} \right] \\
 M_1 &= \frac{1}{4\pi} \left[(2z+x_1) e^{-z} + \frac{\alpha+\beta}{1+\beta} e^z \right. \\
 &\quad \left. + Q_1 \left\{ \frac{1-\beta}{\alpha-\beta} e^{-z} - (2z-x_1) e^z \right\} \right] \\
 N_1 &= \frac{1}{4\pi} \left[(2z+1) e^{-z} - \frac{\alpha+\beta}{1+\beta} e^z + Q_1 \left\{ \frac{1-\beta}{\alpha-\beta} e^{-z} + (2z-1) e^z \right\} \right] \\
 P_1 &= \frac{1}{4\pi} \left[(1-2z) e^{-z} - \frac{\alpha+\beta}{1+\beta} e^z + \right. \\
 &\quad \left. Q_1 \left\{ -\frac{1-\beta}{\alpha-\beta} e^{-z} + (2z+1) e^z \right\} \right] \\
 R_1 &= \frac{1}{4\pi} \left[(2z-3) e^{-z} - \frac{\alpha+\beta}{1+\beta} e^z + Q_1 \left\{ \frac{1-\beta}{\alpha-\beta} e^{-z} + (2z+3) e^z \right\} \right] \\
 L_2 &= \frac{(1-\alpha)}{4\pi(1+\beta)(\alpha-\beta)} [(2z-x_2)(\alpha-\beta) + Q_1(1+\beta)] e^{-z} \\
 M_2 &= \frac{(1-\alpha)}{4\pi(1+\beta)(\alpha-\beta)} [(2z+x_2)(\alpha-\beta) + Q_1(1+\beta)] e^{-z} \\
 N_2 &= \frac{(1-\alpha)}{4\pi(1+\beta)(\alpha-\beta)} [-(2z+1)(\alpha-\beta) - Q_1(1+\beta)] e^{-z} \\
 P_2 &= \frac{(1-\alpha)}{4\pi(1+\beta)(\alpha-\beta)} [(1-2z)(\alpha-\beta) - Q_1(1+\beta)] e^{-z}
 \end{aligned}$$

$$\begin{aligned}
 R_2 &= \frac{(1-\alpha)}{4\pi(1+\beta)(\alpha-\beta)} [(2z-3)(\alpha-\beta) + Q_1(1+\beta)] e^{-z} \\
 B_0 &= (\alpha-\beta)(1+\Gamma x_2) \{-2\xi H(1+\beta) + (1-\beta) - (\alpha-\beta) e^{-2\xi H}\} / \Delta \\
 Q_0 &= -\frac{(1+\beta) e^{2\xi H} - 2\xi H(\alpha-\beta) - (\alpha+\beta)}{-2\xi H(1+\beta) + (1-\beta) - (\alpha-\beta) e^{-2\xi H}} \\
 D_1(\xi, y) &= \frac{1}{4\pi} [(2\xi y + 2\xi H - x_1) e^{-\xi y} - e^{\xi(y+2H)} + Q_0 \{ e^{-\xi(y+2H)} \\
 &\quad + (2\xi y + 2\xi H + x_1) e^{\xi y} \}] \\
 E_1(\xi, y) &= \frac{1}{4\pi} [(2\xi y + 2\xi H + x_1) e^{-\xi y} + e^{\xi(y+2H)} + Q_0 \{ e^{-\xi(y+2H)} \\
 &\quad + (-2\xi y - 2\xi H + x_1) e^{\xi y} \}] \\
 F_1(\xi, y) &= \frac{-1}{4\pi} [(2\xi y + 2\xi H + 1) e^{-\xi y} - e^{\xi(y+2H)} + Q_0 \{ e^{-\xi(y+2H)} \\
 &\quad + (2\xi y + 2\xi H - 1) e^{\xi y} \}] \\
 G_1(\xi, y) &= \frac{1}{4\pi} [(-2\xi y - 2\xi H + 1) e^{-\xi y} - e^{\xi(y+2H)} \\
 &\quad + Q_0 \{ -e^{-\xi(y+2H)} + (2\xi y + 2\xi H + 3) e^{\xi y} \}] \\
 H_1(\xi, y) &= \frac{1}{4\pi} [(2\xi y + 2\xi H - 3) e^{-\xi y} - e^{\xi(y+2H)} + Q_0 \{ e^{-\xi(y+2H)} \\
 &\quad + (2\xi y + 2\xi H + 3) e^{\xi y} \}] \\
 D_2(\xi, y) &= \frac{1}{\pi} [2\xi H - (2\xi y - x_2)(e^{2\xi H} - 1) + Q_0 \{ 2\xi H(2\xi y - x_2) \\
 &\quad + (e^{-2\xi H} - 1) \}] e^{-\xi y} \\
 E_2(\xi, y) &= \frac{1}{4\pi} [2\xi H - (2\xi y + x_2)(e^{2\xi H} - 1) + Q_0 \{ 2\xi H(2\xi y + x_2) \\
 &\quad + (e^{-2\xi H} - 1) \}] e^{-\xi y} \\
 F_2(\xi, y) &= \frac{1}{4\pi} [-2\xi H + (2\xi y + 1)(e^{2\xi H} - 1) - Q_0 \{ 2\xi H(2\xi y + 1) \\
 &\quad + (e^{-2\xi H} - 1) \}] e^{-\xi y} \\
 G_2(\xi, y) &= \frac{1}{4\pi} [-2\xi H + (2\xi y - 1)(e^{2\xi H} - 1) - Q_0 \{ 2\xi H(2\xi y \\
 &\quad - 1) + (e^{-2\xi H} - 1) \}] e^{-\xi y} \\
 H_2(\xi, y) &= \frac{1}{4\pi} [2\xi H - (2\xi y - 3)(e^{2\xi H} - 1) - Q_0 \{ 2\xi H(2\xi y - 3) \\
 &\quad + (e^{-2\xi H} - 1) \}] e^{-\xi y} \\
 K_I'(s, x) &= 2(1-\alpha) \int_0^\infty [\{ -(1+\Psi_1) + (\alpha-\Psi_2) e^{-2\xi H} \} \cos \\
 &\quad \eta(x-s-t) + f_1 \{ (\Psi_1-\beta) + (\beta-\Psi_2) e^{-2\xi H} \} \sin \\
 &\quad \eta(x-s-t)] e^{\eta(H-\xi)} / \Delta d\eta \\
 K_I''(s, x) &= 2(1-\alpha) \int_0^\infty [\{ -(\beta+\Psi_1) + (\beta+\Psi_2) e^{-2\xi H} \} \sin \\
 &\quad \eta(x-s-t) + f_1 \{ -(\Psi_1+1) + (\alpha+\Psi_2) e^{-2\xi H} \} \cos \\
 &\quad \eta(x-s-t)] e^{\eta(H-\xi)} / \Delta d\eta \\
 K_I^P(\xi, x) &= -(1-\alpha^2) \int_0^\infty \Psi_3(\eta) / \Delta \sin \eta(\xi-x) d\eta \\
 K_I^D(\xi, x) &= -(1-\alpha^2) \int_0^\infty \Psi_4(\eta) / \Delta \sin \eta(\xi-x) d\eta
 \end{aligned}$$

where,

$$\begin{aligned}
 z &= \xi y \\
 \Psi_1 &= (1+\beta) \xi H, \quad \Psi_2 = (\alpha-\beta) \xi H \\
 \Psi_3 &= -2(1+\beta)^2 \xi^2 H^2 - 2\beta + \beta(1+\alpha) e^{-2\xi H} \\
 \Psi_4 &= 2(1+\beta) \xi H \{ (1+\beta) \xi H - (1-\beta) \} + 1 + \beta^2 - (\alpha+\beta^2) e^{-2\xi H} \\
 \Delta &= (1-\beta^2) e^{2\xi H} + (\alpha^2-\beta^2) e^{-2\xi H} - 2(\alpha-\beta^2) \\
 &\quad - 4\xi^2 H^2 (\alpha-\beta)(1+\beta) \\
 \alpha &= \frac{\Gamma(x_0+1) - (x_1+1)}{\Gamma(x_0+1) + (x_1+1)}, \quad \beta = \frac{\Gamma(x_0-1) - (x_1+1)}{\Gamma(x_0+1) + (x_1+1)}
 \end{aligned}$$

Here, α and β are Dundurs' constants(Dundurs, 1969; Dundurs, 1970).